17D.4 COLLABORATION OF INTRASEASONAL OSCILLATION AND SYNOPTIC-SCALE DISTURBANCES IN THE SOUTH CHINA SEA SUMMER MONSOON ONSET

H. W. Tong, and J. C. L. Chan *

Laboratory of Atmospheric Research, Dept. of Physics & Mat. Sci.

City University of Hong Kong

1. INTRODUCTION

Numerous studies (e.g. Chen and Chen, 1995) have shown that a northward propagating trough triggers the South China Sea summer monsoon (SCSSM) onset. This trough is usually related to a Madden and Julian Oscillation (MJO; Lawrence and Webster, 2002). On the other hand, from a synoptic point of view, some studies pointed out that a mid-latitude front may be the triggering mechanism of the SCSSM onset (Chang and Chen 1995, Chan et al., 2000). This study attempts to link these two very different time-scale phenomena via a case study of the 1998 SCSSM and numerical simulations

2. DATA

The following data are used: 6 hourly reanalysis of the European Centre for Medium Range Weather Forecasts ERA-40 data set for the period 1 April – 30 June 1998, the daily outgoing longwave radiation (OLR) from the US National Centers for Environmental Prediction (NCEP) for the same period. OLR values lower than 220 W m^{-2} are regarded as deep convection in this study. Both data sets have a horizontal resolution of 2.5^o latitude $\times$ 2.5^o longitude.

3. 1998 SCSSM OBSERVATIONS

3.1. Cold air intrusion events

The time-latitude cross-section of surface temperature averaged between 110-120^{o}E (Fig.1) shows a strong cold air intrusion event

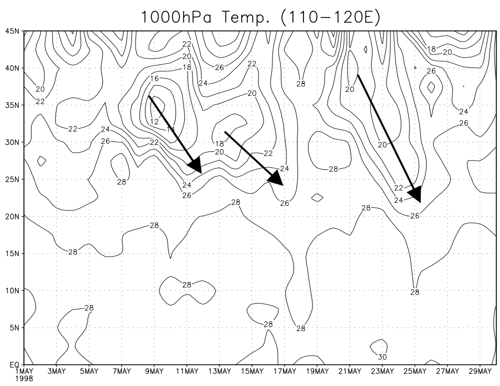

Fig .1. Time-latitude cross-section of near surface temperature averaged between 110-120^{o}E. Unit: ^{o}C. Solid arrows indicate the cold air intrusion events.

* *Corresponding author address: J. C. L. Chan, Department of Physics and Materials Science, City University of Hong Kong, 83 Tat Chee Ave., Kowloon, Hong Kong, China.*
E-mail: Johnny.Chan@cityu.edu.hk

occurring around 22-25 May which eventually led to the SCSSM onset (Chan et al, 2000). However, it was not the only cold air intrusion event in that month. The first event occurred between 9-11 May and the second event was between 14-17 May. Synoptic charts (not shown) show that the first two events could not reach the northern South China Sea (NSCS) because of the blocking by the subtropical high. Unlike the first two events, the subtropical high started to weaken on 21 May. The cold air could then move all the way down to NSCS and trigger the onset.

3.2. Westerly surge

The MJO was strong in 1998 (Fig. 2a). Easterly (westerly) winds are induced ahead (behind) of the heating centre as a Kelvin (Rossby) wave response (Fig. 2b). This not only occurs over the equatorial latitude band, but also occurs over the 5-15^{o}N latitude band (Fig. 2c). The abrupt low-level zonal wind shift from easterly to westerly over the SCS domain is clearly associated with the MJO (Fig. 2d). The acceleration of the westerly winds associated with the approach of mid-latitude front can be seen but is quite limited.

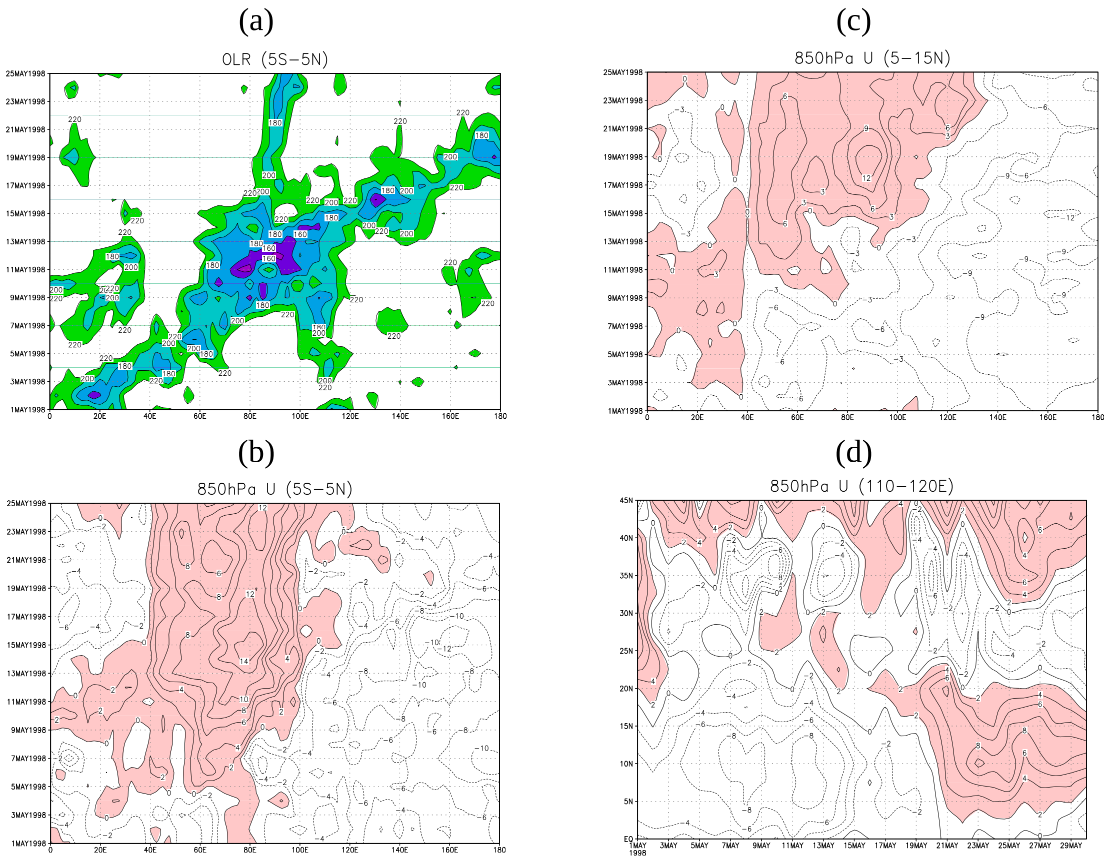

Fig. 2. Time-longitude cross-section of a) OLR (unit: W m^{-2}; values < 200 W m^{-2} are shaded), b) 850-hPa zonal wind (unit: m s^{-1}; westerly winds are shaded) averaged between 5^{o}S-5^{o}N. c) Same as b), but averaged between 5-15^{o}N. d) Time-latitude cross-section of 850-hPa zonal wind averaged between 110-120^{o}E. Values > 2 m s^{-1} are shaded

3.3. Sudden increase in precipitation

The time-longitude cross-section of upper-level divergence (not shown) shows that there is an eastward propagation of divergence centre which is possibly related to the MJO again.. The time series of 30-60-day filtered 200-hPa divergence and OLR (not shown) shows that deep convection is highly suppressed when the upper-levels are dominated by convergence prior to the onset. On the contrary, the deep convection outbreak on 25 May is supported by the upper-level divergence. Chan et al. (2000) have clearly shown that the outbreak of convection over the central SCS is associated with the approach of a mid-latitude front. The front may provide a lifting mechanism for the final trigger, but the MJO-induced upper-level divergence provides a necessary condition for the outbreak.

4. NUMERICAL SIMULATIONS

4.1. Model

To ascertain further the findings in the case study, numerical simulations are carried out using a regional climate model. The model was first developed by the National Climate Center in China based on the RegCM2. Chan et al. (2004) modified the model (hereafter RegCM_SCS) to simulate the SCSSM onset process. The reader is referred to Chan et al. 2004 for a detailed description of the RegCM_SCS.

The initial atmospheric conditions and lateral boundary conditions are taken from the ERA-40 data set. The sea surface temperature data are taken from the NOAA Optimum Interpolation SST V2 weakly mean data with 1-degree latitude-longitude resolution. This weekly mean data are then linearly interpolated to daily values.

The experiments are initiated from 0000UTC on 1 April, 1998 and integrated continuously through 30 June. 1998.

4.2. Control run

Large-scale features such as the penetration of westerly winds from the Bay of Bengal region and even the cold air intrusion events are well simulated (not shown). However, a closer look at the time-latitude cross-section of the 850-hPa zonal wind shows that the timing of the abrupt shift of zonal wind direction is on 13 May which is a week ahead of the actual onset (not shown).

Another problem with the control run is the poor simulation of the MJO. The time-longitude cross-section (not shown) shows no sign of eastward propagation of convection at all.

4.3 Moving heat source experiment

Given the significance of the MJO shown in the case study, it is possible that the early onset in the model is due to the poor simulation of the MJO. To see if it is the case, an idealized moving heat source that mimics the eastward propagation of the MJO is imposed. In the vertical, the heating is peaked at the 400-hPa surface. On the horizontal, the moving heat source has an elliptical shape and a maximum heating rate of $8^{o}C\ day^{-1}$ on the 400-hPa surface and an eastward moving speed of $8\ m\ s^{-1}$.

The time-longitude cross-section of the

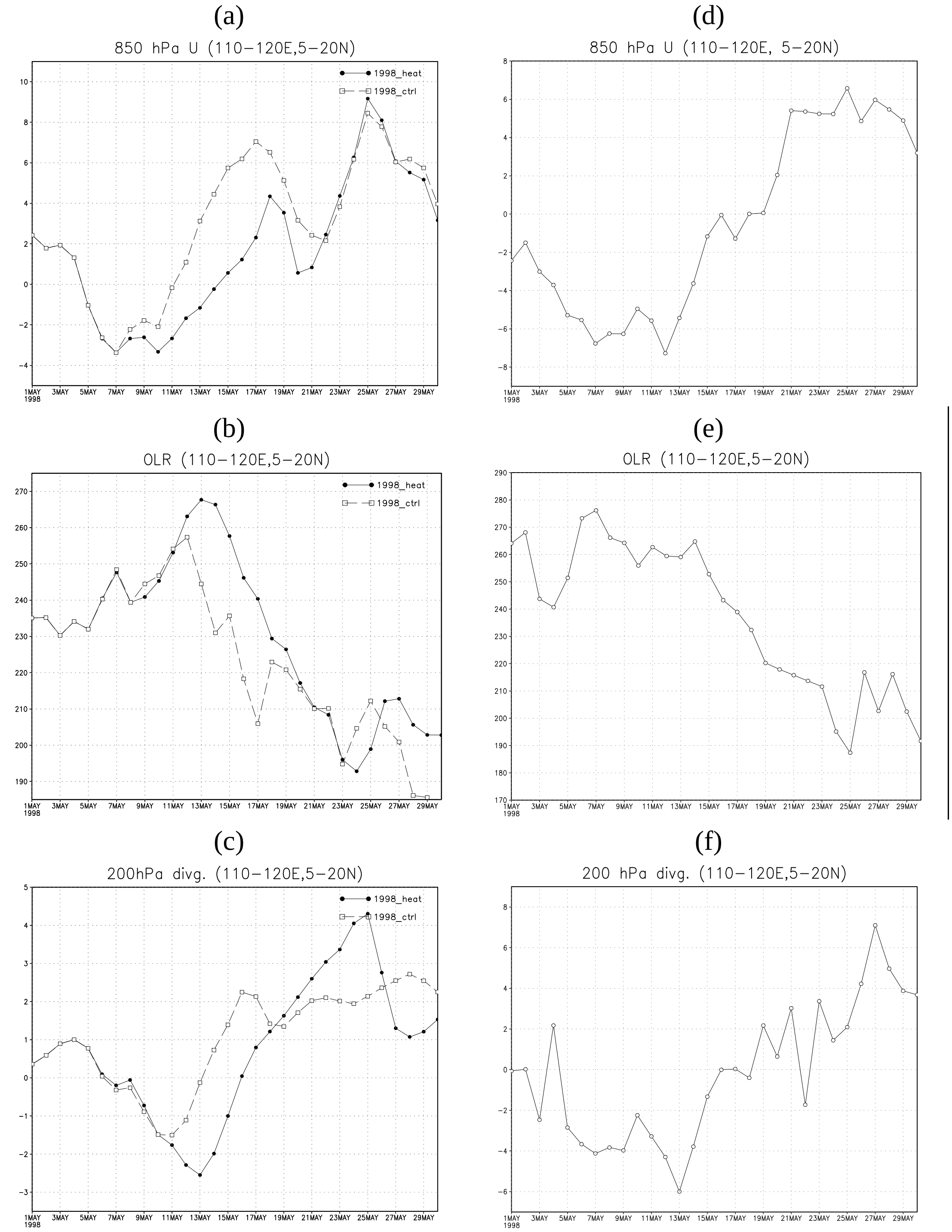

Fig. 3. Time series of a) 850-hPa zonal wind (unit: m s^{-1}), b) OLR (unit: W m^{-2}) and c) 200-hPa divergence (unit: 1 × 10^{-6} s^{-1}) averaged between 110-120°E, 5-20°N. Solid lines are for the moving heat source experiment and dashed lines are for the control run. d), e) and f) Same as a), b) and c) respectively, but from ERA-40 data set.

OLR averaged between 5°S-5°N (not shown) shows that the MJO is well-simulated. Compared with the control run, the onset of westerlies is delayed in the moving heat source experiment (Fig. 3a). The westerly winds on 15-17 May in the control run are associated with a mesoscale cyclone along the south China coast. This mesoscale cyclone also exists in the moving heat source experiment (not shown). However, with the presence of moving heat source and its associated easterlies, the westerly winds associated with the mesoscale cyclone are reduced.

For deep convection, the main effect of the moving heat source is to suppress the convective activities prior to the onset. In the control run, deep convection emerges as early as 16 May, which is apparently associated with the mesoscale cyclone. In the moving heat source experiment, the outbreak of deep convection is delayed to 20 May which is closer to observation. This could be explained by the anomalous upper-level convergence induced in the moving source experiment prior to the 16 May (Fig. 3c) which possibly prohibits the development of deep convection associated with the mesoscale cyclone. This experiment shows that the outbreak of convection would not occur without the support of upper-level divergence, even though a mesoscale cyclone may exist along the south China coast.

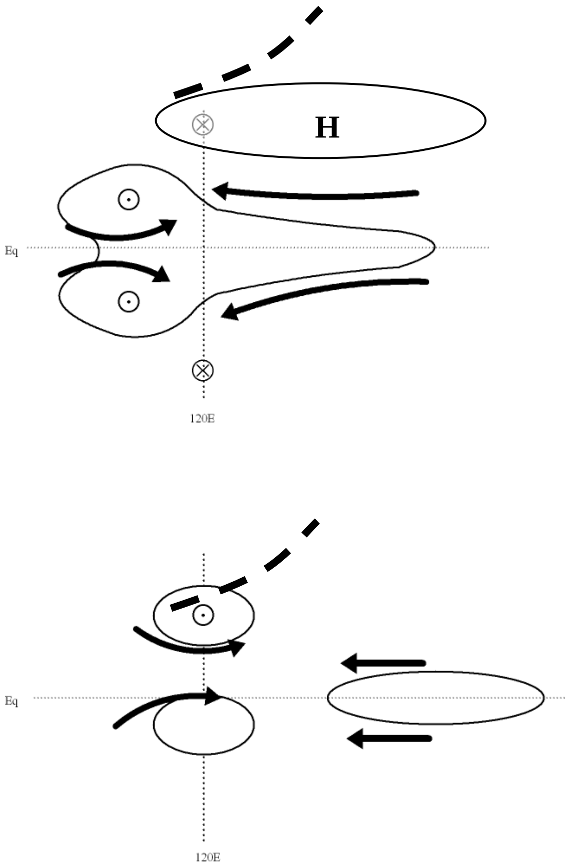

Fig. 4. Schematic representation of the effect of the MJO and mid-latitude fronts on SCSSM prior to (upper panel) and during (lower panel) the onset. Thick arrows represent the wind direction at low levels. ⊙ denotes the area of upper-level divergence and ⊗ denotes the area of upper-level convergence. The thick dashed line denotes the mid-latitude fronts.

5. SUMMARY

Based on the case study and numerical experiments, the sequence of the 1998 SCSSM onset is summarized in the schematic diagram (Fig. 4). The main features include:

1) Prior to the onset, a MJO episode develops over the equatorial Indian Ocean. Low-level easterly winds are induced ahead of the heating center and westerlies at its wake. Its associated upper-level divergence dominates the central SCS and hence the convective activities are highly suppressed. Meanwhile, two cold air intrusion events occur over China. However, they are blocked by the subtropical high and as a result cannot enter the SCS.

2) When the MJO moves eastward, the low-level easterly–westerly shift also moves eastward. This causes a large-scale directional change of zonal wind over the SCS domain on 21 May. Associated with the MJO, a Rossby wave

response propagates northward and in situ weakens the subtropical high over the SCS. Meanwhile, a cold front develops over China. Unlike the previous two, this front could move all the way down to the NSCS due to the weakened subtropical high. This lifts the air up and deep convection is further enhanced by the upper-level divergence. The directional change of low-level zonal wind and the outbreak of deep convection over the central SCS signify the full onset.

Acknowledgements. The research of this study forms part of the Master of Philosophy research of the first author, which was supported by a Postgraduate Research Studentship from the City University of Hong Kong. Partial support was also provided by the grant from City University of Hong Kong under Grant No. 7200098.

6. REFERENCES

Chan, J. C. L., Y. Wang., and J. Xu, 2000: Dynamic and thermodynamic characteristics associated with the onset of 1998 South China Sea Summer monsoon. *J. Meteor. Soc. Japan*, **78**, 367-380.

____, Y. Liu, K. C. Chow, Y. Ding, W. K. M. Lau, and K. L. Chan, 2004: Design of a regional climate model for the simulation of south China summer monsoon rainfall. *J. Meteor. Soc. Japan*, **82**, 1645-1665

Chang, C.-P. and G. T.-J., Chen, 1995: Tropical circulations associated with southwest monsoon onset and westerly wurges over the South Chin Sea. *Mon. Wea. Rev*., **123**, 3254-3267.

Chen, T.-C., and J.-M. Chen, 1995: An observational study of the South China Sea Monsoon during the 1979 summer: onset and life cycle. *Mon Wea. Rev*., **123**, 2295-2317.

Lawrence, D. M., and P. J. Webster, 2002: The boreal summer intraseasonal oscillation: Relationship between northward and eastward movement of convection. *J. Atmos. Sci*., **59**, 1593-1606